AEROMAGNETIC SURVEY OF THE AMARGOSA DESERT, NEVADA AND CALIFORNIA: A TOOL FOR UNDERSTANDING NEAR-SURFACE GEOLOGY AND HYDROLOGY

By Richard J. Blakely[1], Victoria E. Langenheim[1], David A. Ponce[1], and Gary L. Dixon[2]

Open-File Report 00–188

Prepared in cooperation with the Nevada Operations Office,
U.S. Department of Energy (Interagency Agreement
DE-AI08-96NV11967)

2000

U.S. DEPARTMENT OF THE INTERIOR
U.S. GEOLOGICAL SURVEY

[1]U.S. Geological Survey, Mail Stop 989, 345 Middlefield Road, Menlo Park, CA 94025
[2]U.S. Geological Survey, Mail Stop 582, 6770 S. Paradise Road, Las Vegas, NV 89119

CONTENTS

ILLUSTRATIONS

ABSTRACT

A high-resolution aeromagnetic survey of the Amargosa Desert and surrounding areas provides insights into the buried geology of this structurally complex region. The survey covers an area of approximately 7,700 km^2 (2,970 mi^2), extending from Beatty, Nevada, to south of Shoshone, California, and includes parts of the Nevada Test Site and Death Valley National Park. Aeromagnetic flight lines were oriented east-west, spaced 400 m (0.25 mi) apart, and flown at an altitude of 150 m (500 ft) above terrain, or as low as permitted by safety considerations. Characteristic magnetic anomalies occur over volcanic terranes, such as Yucca Mountain and the Greenwater Range, and over Proterozoic basement rocks, such as Bare Mountain and the Black Mountains. Linear magnetic anomalies caused by offsets of volcanic rocks permit detailed mapping of shallow faults in volcanic terranes. Of particular interest are subtle anomalies that overlie alluvial deposits at Devils Hole and Pahrump Valley. Alignments of springs along magnetic anomalies at these locales suggest that these anomalies are caused by faults that cut the alluvium, displace magnetic rocks at depth, and eventually influence ground-water flow. Linear magnetic anomalies over the Funeral Mountains appear to coincide with a prominent set of north-northeast-striking faults that cut the Precambrian Stirling Quartzite, rocks that are typically nonmagnetic. The position and orientation of these anomalies with respect to springs north of Furnace Creek suggest that the faults may act as conduits for the flow of water from the north into Death Valley, but the mineralogical cause of the anomalies is unknown.

INTRODUCTION

This report summarizes the acquisition, data processing, and preliminary interpretation of high-resolution aeromagnetic data from the Amargosa Desert and surrounding areas of Nevada and California. The survey was flown during the summer of 1999 with funding from Nye and Clark Counties, Nevada; Inyo County, California; and the National Park Service. The survey was designed to assist ongoing geologic mapping and ancillary geophysical studies focused on understanding subsurface lithology and structure, important for models of tectonic evolution and ground-water flow. The interpretation presented here is regional in scope; more quantitative and site-specific investigations are planned in the future.

ABOUT THE METHOD

Geologic structures (like faults and folds) may produce small magnetic fields that distort the main magnetic field of the earth (fig. 1). These anomalies can be detected by measuring the earth's magnetic field on or near the surface of the ground. By analyzing magnetic measurements, geophysicists are able to learn about geologic structures, even though the structures may be concealed entirely below the earth's surface (for example, Dobrin and Savit, 1988; Blakely, 1995). Magnetic measurements are usually made from aircraft flown along closely spaced, parallel flight lines. Additional flight lines are flown in the perpendicular direction to assist in data processing. These measurements then are processed into a digital aeromagnetic map. Assisted by computer programs, a geologic interpretation or model is developed from these data, incorporating geologic mapping and other geophysical information, such as gravity or seismic-reflection data, where available.

GEOLOGIC SETTING

The survey covers an area of approximately 7,700 km^2 (2,970 mi^2), extending from Beatty, Nevada, to south of Shoshone, California (fig. 2). The area includes most of the Amargosa Desert and Pahrump Valley, including the towns of Beatty, Amargosa Valley, Death Valley Junction, Pahrump, and Shoshone. It also covers parts of the Nevada Test Site and Death Valley National Park.

The survey area lies within the western part of the Basin and Range physiographic province, which is characterized by broad, relatively flat basins surrounded by mountain ranges.

Pre-Cenozoic rocks of diverse age and lithology (fig. 3) underlie most of the ranges in the study area. Paleozoic carbonate rocks (limestone and dolomite) are exposed in the Funeral Range, Spring Mountains, and other ranges, and underlie parts of the alluvial basins as well. Carbonate rocks are believed to be an important aquifer in this part of the Basin and Range (Winograd and Thordarson, 1975; Dettinger, 1989; Laczniak and others, 1996; McKee, 1997).

Several authors (for example, Stewart, 1983; Wernicke and others, 1988; Hamilton, 1988) have concluded that large crustal extensions during the last 15 m.y. were accommodated on regionally continuous detachment surfaces lying beneath most of this region. Rocks of the upper plate, above the detachment surface, are characterized as permeable, brittle, and fractured carbonate rocks (McKee, 1997). Rocks of the lower plate, on the other hand, are highly metamorphosed, ductilely deformed, and could act as impediments to the flow of ground water (McKee, 1997). The detachment surface crops out in the Funeral Range and at Bare Mountain, exposing Proterozoic lower-plate siliceous rocks formerly buried to middle crustal depths (Hamilton, 1988).

Some of the mountains and the basins that separate them contain variable thicknesses of sedimentary and volcanic deposits, Oligocene and younger in age. These include fluvial conglomerate, sandstone, siltstone, lacustrine claystone and limestone, volcanic pyroclastic deposits of various types, and lava flows.

Tertiary volcanism was important in the Great Basin, especially the eruption of voluminous ash flows that lead to the formation of large collapse calderas. Thick Tertiary volcanic sections composed mostly of welded tuffs from the southwest Nevada volcanic field (a group of collapse calderas north of the study area) extend from the north into the northern and northwestern parts of the area (fig. 3). Volcanic rocks also dominate the landscape at Brown Peak and the Greenwater Range in the southwestern part of the study area.

Magnetic lithologies

Volcanic rocks are the most ubiquitous magnetic lithology of this region, and we expect high-amplitude, short-wavelength anomalies over volcanic terranes along the northern part of the survey and over the Greenwater Range and Greenwater Valley. Volcanic rocks in this region typically include ash-flow tuffs, lava flows, and layered volcanogenic units of many types, which individually have uniform direction of magnetization. Steeply dipping faults that offset these units often produce magnetic anomalies that appear as linear trends on aeromagnetic maps (for example, Bath and Jahren, 1984; Ponce, 1996).

Most Paleozoic carbonate and siliceous stratified rocks of this region are relatively nonmagnetic, with one exception: The argillite member of the Devonian- to Mississippian-aged Eleana Formation, exposed in the Calico Hills, is highly magnetic. Baldwin and Jahren (1982) reported an average bulk magnetization of 3.89 A/m for this argillite rock based on samples recovered from a drill hole in the Calico Hills. For comparison, samples of volcanic rocks from the same area (tuff, tuffaceous beds, and rhyolite intrusions) had magnetizations ranging from 0 to 2.6 A/m (Baldwin and Jahren, 1982). (See Blakely (1995) for a discussion of magnetic units.)

Precambrian rocks in the study area sometimes produce distinctive magnetic anomalies. One of the most prominent anomalies in Nevada, centered over Charleston Peak, has been interpreted as being caused by a concealed upwarp of Precambrian basement, assumed to be more magnetic than overlying rocks (Blank, 1987). Clastic siliceous rocks of the Proterozoic Wood Canyon Formation exposed at Bare Mountain (Monsen and others, 1992) have significant magnetizations and will be discussed below. Magnetic anomalies over the Black Mountains in Death Valley National Park have been interpreted as being caused by Precambrian metamorphic rocks (Blakely and others, 1999).

Most of the study area is covered with relatively nonmagnetic alluvial deposits, and alluvium-filled basins are expected to produce only subdued aeromagnetic patterns. As discussed subsequently, several interesting exceptions occur in the Amargosa Desert and Pahrump Valley.

DATA ACQUISITION AND PROCESSING

The aeromagnetic survey was conducted by Sander Geophysics Limited (SGL) under contract to the U.S. Geological Survey. SGL is headquartered in Ottawa, Canada, and has many years of experience in acquiring and processing aeromagnetic data. Data acquisition and processing were accomplished under guidelines established by the U.S. Geological Survey over the last several decades. Weekly reports were submitted to the USGS, and preliminary data were provided for evaluation at regular intervals. The Project Chief (R. Blakely) made one visit during field operations to monitor progress.

The aeromagnetic data were acquired with a Britten-Norman Islander BN2B-21, a fixed-wing aircraft with exceptional climb and descent capabilities. The airborne magnetic sensor was a cesium-vapor magnetometer located at the tip of a fiberglass stinger. A theoretical flight surface, based on a digital topographic model, was computed in advance of the survey, and a real-time, differentially corrected Global Positioning System (GPS) was used during flight to maintain this theoretical surface. Flight lines were oriented east-west, spaced 400 m (0.25 mi) apart, and flown at an altitude of 150 m (500 ft) above terrain, or as low as permitted by the Federal Aviation Administration and safety considerations. North-south control lines were spaced 2.3 km (1.4 mi) apart. Total flight distance was 23,333 km (14,502 mi). Figure 4 shows flight path locations.

Base station magnetometers were deployed at Henderson Field (near Las Vegas and about 75 km east of Pahrump) and at Beatty, and at least one of these magnetometers was in operation at all times of the survey. The fixed magnetometers measured the time-varying magnetic field and have two important functions: They record the normal daily changes of the external field (diurnal variation), which are subsequently subtracted from the aeromagnetic data, and they track the onset and dissipation of magnetic storms. Airborne operations were interrupted if magnetic storm activity exceeded limits established by the U.S. Geological Survey. These limits are as follows: (1) 5 nT for monotonic changes during any 5 minute period, (2) 2 nT for pulsations with periods of 5 minutes or less, (3) 4 nT for pulsations with periods between 5 and 10 minutes, and (4) 8 nT for pulsations with periods between 10 and 20 minutes. Base-station instruments were cesium-vapor magnetometers, identical to the airborne sensor. Time between aircraft and base stations was synchronized with GPS time.

Preliminary data processing was performed by SGL. This included removal of diurnal fields, subtraction of the International Geomagnetic Reference Field (Blakely, 1995), navigational corrections, and adjustment of total-field values between crossings of flight lines and tie lines. A preliminary version of the completed survey was provided to the USGS for evaluation in November 1999. Incidental problems were discussed with SGL and subsequently rectified. Final data were delivered in December 1999.

AEROMAGNETIC MAP AND DERIVATIVE PRODUCTS

Figure 5 shows the aeromagnetic survey, where color scale indicates the intensity of the earth's magnetic field relative to a global standard (the International Geomagnetic Reference Field updated to the date of the survey). Volcanic regions produce distinctive magnetic anomalies, high in amplitude and short in wavelength. These are particularly evident over the southwest Nevada volcanic field (Yucca Mountain, Calico Hills) at the northeastern corner of the map and over the Greenwater Range and Greenwater Valley along the southwestern edge of the map. Many of the volcanic anomalies are linear for distances of 10 to 20 km, in some cases indicating faults that have offset sub-horizontal volcanic units at shallow depth (Bath and Jahren, 1984; Ponce, 1996).

Precambrian metamorphic rocks cause other anomalies, notably over Bare Mountain and the Spring Mountains. The broad, high-amplitude anomaly at the southeastern corner of the map (fig. 5) forms the western flank of a magnetic high centered approximately over Charleston Peak (outside the survey boundary). The source of this anomaly is completely concealed but has been interpreted to be a domal-form upwarp of Precambrian rocks more magnetic than overlying rocks (Blank, 1987).

Of particular interest are subtle anomalies that overlie alluvial deposits, notably the region centered about 15 km (9 mi) north of Devils Hole, the region 10 km (6 mi) northeast of Death Valley Junction, and the region along the Nevada-California state line near the southern edge of the map (fig. 5). Alluvium is typically only weakly magnetic, and some of these anomalies may originate from volcanic or other magnetic rocks concealed beneath the surface. Others may be caused by alteration along fault zones or by concentration of magnetite during fluvial reworking of alluvial deposits.

Magnetic anomalies are subdued over most Paleozoic exposures, such as those over the Funeral Range, Nopah Range, and Resting Spring Range. Some exceptions will be discussed in the subsequent section.

Subtle magnetic anomalies exist in the original aeromagnetic data that are not obvious in figure 5. The magnetic field over thick alluvial sections throughout most of the Amargosa Desert, for example, is essentially featureless as portrayed in figure 5, although very low-amplitude magnetic anomalies can be seen on careful examination. (Note, for example, the region between latitudes 36°15'N. and 36°30'N., and between longitudes 116°00'W. and 116°15'W.)

The aeromagnetic data are of sufficient detail to permit the application of well-established processing and filtering techniques that emphasize some of the subtle features. Figures 6 and 7 show the aeromagnetic data processed in ways to assist our interpretation. Figure 6 shows "residual magnetic anomalies", computed with a technique that emphasizes shallow magnetic sources. This map was derived by analytically continuing the aeromagnetic map to a slightly higher surface (Blakely, 1995) and subtracting that result from the original data. Figure 7 shows magnetic contacts, automatically computed from the aeromagnetic data (Blakely and Simpson, 1986). This calculation assumes that magnetic contacts are vertical; calculated positions will be shifted slightly over contacts that are not vertical. Both of these maps (figs. 6 and 7) were important tools in developing the interpretation that follows.

DATA AVAILABILITY

Digital versions of the Amargosa aeromagnetic survey can be downloaded from anonymous FTP (File Transfer Protocol) directory,

ftp://geopubs.wr.usgs.gov/pub/open-file/of00-188/data.

The following ASCII files are available:

amargosa.xyz.gz—discrete point measurements along flight lines,
amargosa.gxf.gz—projected grid of the entire survey, and
amargosa.info—a detailed description of the data.

Each point measurement includes latitude, longitude, altitude (based on radar altimetry), total-field magnetic anomaly, and various other items. The digital grid was computed by transforming the flight-line point data to Universal Transverse Mercator projection, then using a minimum-curvature algorithm to interpolate values to rectangular grid intersections. Grid intersections are spaced 100 m apart. The gridded data are in Geosoft Grid Exchange Format (GXF), a standard ASCII format for exchanging gridded data among different software systems. GXF is described more fully in the informational file located in the anonymous FTP directory named above. To speed file transfers, all files have additionally been compressed into the public-domain "gzip" format (as indicated by the suffix .gz). Gzip format is commonly used on PC DOS, PC Windows, Macintosh, and Unix platforms. It too is described more fully in the informational file located in the anonymous FTP directory.

INTERPRETATION

Figure 8 and plate 2 show a preliminary interpretation of the aeromagnetic survey. This map-based interpretation emphasizes (1) magnetic lineaments that in some cases may be shallow faults and (2) magnetic patterns that indicate underlying lithologies. It is regional and qualitative in scope. Letter labels on figure 8 indicate specific anomalies and patterns discussed below. Figure 9 shows the interpreted magnetic lineaments on the generalized geology map, and figure 10 compares the magnetic lineaments with depth to pre-Tertiary basement rocks. Depths to pre-Tertiary rocks were derived from a three-dimensional gravity inversion, constrained by geologic mapping, well information, and seismic-reflection data (Blakely and others, 1998). The following discussion relies heavily on previously published interpretations of aeromagnetic and ground-magnetic data from this region (Ponce, 1984, 1993, 1996; Ponce and Langenheim, 1994; Ponce and others, 1995; Langenheim, 1995; Langenheim and others, 1993; Louie and others, 1998; Connor and others, 2000).

Nevada Test Site and Highway 95 region

The distinctive pattern of aeromagnetic anomalies north of Highway 95 (fig. 5, plate 1) is caused principally by Miocene and younger volcanic rocks underlain in some areas by highly magnetic, older metamorphic or plutonic rocks. The north- to northeast-striking linear nature of the anomalies over this volcanic terrane is caused in part by shallow, near-vertical faults that offset relatively flat-lying volcanic units, such as the normally polarized Topopah Spring Tuff (for example, Bath and Jahren, 1984; Ponce, 1996). These faults include the Solatario Canyon fault, (S, fig. 8), Paintbrush Canyon fault (P, fig. 8), Ghost Dance fault (G, fig. 8), and Bow Ridge fault (B, fig. 8). Linear magnetic anomalies follow Yucca Wash (Y, fig. 8) and also may indicate faults in this area (Bath and Jahren, 1984; Ponce and Langenheim, 1994).

The linear appearance of Fortymile Wash (FW, fig. 8) suggests structural control, but the lack of magnetic expression in ground-based magnetic profiles led Ponce and others (1992) to conclude that shallow volcanic units at Fortymile Wash do not have significant vertical offsets on faults. Their conclusion is supported by the high-resolution aeromagnetic data (figs. 5 and 6, plate 1): No linear anomalies are associated with the topography of Fortymile Wash, which precludes significant vertical offsets of the shallow volcanic section. We cannot rule out the possibility, however, that fault displacements have juxtaposed rocks of similar magnetic properties.

Many other north- to northeast-striking lineaments are identified but unlabeled on fig. 8. We suspect that some of these reflect faulted volcanic units. It is important to recognize, however, that other explanations are possible, such as abrupt changes in subsurface lithology or topography in magnetic terrane.

A northeast-striking lineament (Z, fig. 8) obliquely crosses Yucca Mountain, coincides with the Stagecoach Road fault (Simmonds and others, 1995; Rosenbaum and others, 1991), and appears to offset a number of north-south anomalies in a right-lateral sense. Anomalies south of lineament Z are rotated about 30° clockwise with respect to anomalies northward. Paleomagnetic investigations of Miocene ash flow tuffs from this area (Rosenbaum and others, 1991) found that southern Yucca Mountain has undergone vertical-axis, clockwise rotations of about 30° since 13 Ma with respect to northern Yucca Mountain. The magnetic anomalies north and south of lineament Z apparently reflect this structural rotation.

Three east-west magnetic patterns suggest the presence of east-west structures beneath the volcanic terrane. The most pronounced of these (X1, fig. 8) generally corresponds to the southern extent of Tertiary volcanic exposures (fig. 9, plate 2) and the southern extent of deep basins associated with the southwestern Nevada volcanic field (fig. 10). Most of the north- to northeast-striking lineaments over volcanic exposures to the north terminate abruptly at this east-west lineament. Lineament X1 may simply mark the depositional edge of volcanism, but the linear nature of this discontinuity and its alignment with the southern extent of deep volcanic basins suggest structural control. Perhaps Miocene and younger volcanic units here are truncated by an east-west crustal structure now concealed by even younger alluvial deposits. This interpretation is consistent with ongoing, large-scale geologic mapping and with data from the Nye County Early Warning Drilling Program boreholes (C. Potter and D. Sweetkind, written commun., 1999).

The other two east-west discontinuities (X2 and X3, fig. 8) may indicate pre-Tertiary sources concealed beneath the younger volcanic section. Candidate lithologies include the Eleana Formation; Cretaceous or Tertiary intrusions, such as the Wahmonie granodiorite (Ponce, 1984); or Precambrian basement rocks. The very high-amplitude magnetic anomaly over the Calico Hills is truncated at X3. The Calico Hills are underlain by highly magnetic Eleana Formation (Baldwin and Jahren, 1982). The high magnetization of these metamorphic rocks may be a result of alteration associated with underlying plutons (Baldwin and Jahren, 1982), and it is possible that the anomaly over the Calico Hills is caused in part by intrusions beneath the Eleana Formation. Discontinuities X2 and X3 do not offset or terminate north- to northeast-striking magnetic anomalies that originate from the volcanic section. Therefore, if discontinuities X2 and X3 are faults, they apparently have not been active since Miocene time. We also note that lineament X3 marks the southern margin of a deep sub-basin beneath northern Yucca Mountain (fig. 10).

Paleozoic and Precambrian rocks that underlie Bare Mountain produce characteristic anomalies (BM, fig. 8) distinctly different from anomalies over Miocene and younger volcanic terrane. Individual anomalies are lineated east-northeast and, in some places, overlie steeply dipping exposures of stratified clastic rocks of the Precambrian Wood Canyon Formation (Monsen and others, 1992). This pattern of anomalies ends abruptly along the eastern extent of pre-Tertiary exposures at Bare Mountain, suggesting that the contact here dips steeply to the east. Along the west margin of Bare Mountain, the pattern of anomalies extends a short distance west of pre-Tertiary exposures, and pre-Tertiary rocks probably are located at shallow depth beneath the pediment west of Bare Mountain. A three-dimensional inversion of gravity data (Blakely and others, 1998) also found pre-Tertiary basement at shallow depth in this location (fig. 10).

A broad, high-amplitude magnetic anomaly (E, fig. 8) at the northeastern margin of the aeromagnetic survey is located over Quaternary sedimentary deposits and originates from sources beneath the sediment cover. The anomaly is surrounded by exposures of Tertiary volcanic rocks. These exposures do not produce large magnetic anomalies, however, and the broad nature of the anomaly suggests that it originates from deeper lithologies. Based on similarity with the magnetic anomaly over the Calico Hills, we suggest that anomaly E is caused by the argillite member of the Eleana Formation located at shallow depth.

Carrara fault

A short but prominent magnetic anomaly (C1, fig. 8) strikes northwest directly along Highway 95 and corresponds with a segment of the Carrara fault reported by Connor and others (2000, Plate 3b). Stamatakos and others (1997) concluded that the Cararra fault is an active, first-order fault extending southeastward from just south of Beatty to the southern end of Bare Mountain and perhaps farther south. They inferred on the basis of detailed gravity and magnetic studies that the Cararra fault has both dextral strike-slip and dip-slip displacement, with minimum offsets of 3 km horizontally and 300 m vertically.

The southeastward projection of anomaly C1 intersects an arcuate, northeast-striking anomaly (C2, fig. 8) that does not appear to be offset by the Cararra fault. Therefore, if the Cararra fault is an active structure with significant displacement, it seems unlikely that it extends immediately southeastward from anomaly C1.

Magnetic lineament C3 (fig. 8) strikes southeast from the southern tip of Bare Mountain and terminates near two Nye County Early Warning Drilling Program boreholes (NC-EWDP-1D and NC-EWDP-1S). These boreholes penetrated a fault identified as part of the Carrara fault zone (T. Buqo, written commun., 1999), and magnetic lineament C3 may indicate a specific segment of the Carrara fault. Alternatively, lineament C3 may connect with the Bare Mountain fault that parallels the eastern slopes of Bare Mountain.

The southeastern projection of lineament C3 intersects a northeast-striking anomaly (C7, fig. 8) just southeast of the NC-EWDP-1 boreholes. The northeast-striking anomaly is not offset by C3, however, suggesting that, if lineament C3 is caused by the Carrara fault, the fault does not extend uninterrupted southeast of the intersection of C3 and C7. Anomaly C7 may reflect a fault that has offset the Carrara fault zone in a sinistral sense.

Thus, at two places (C1 and C3, fig. 8) where the Cararra fault has been identified independently, magnetic anomalies suggest that the fault is not a single throughgoing structure. On the other hand, the broad region southwest and south of Bare Mountain is characterized by numerous linear anomalies with northwest (e.g., anomalies C1, C3, C4, C5, and C6) and northeast (e.g., C2 and C7) strike. Perhaps this pattern reflects a complex zone of faults along the western margin of Bare Mountain accommodating predominantly dextral strike-slip displacement.

Rock Valley fault zone and surrounding area

A distinctive band of magnetic anomalies (R, fig. 8) overlies the southwestern part of the Rock Valley fault zone. The magnetic zone is about 5-km wide, with a pronounced central anomaly that sinuates between pre-Cenozoic exposures aligned with similar trend. The Rock Valley fault zone is an oblique fault, with left-lateral strike-slip and north-side-down displacement (O'Leary, 2000). It is considered by Rowley (1998) to be a conjugate fault within the Las Vegas Valley shear zone, a complex, regionally important zone of dominantly right-lateral deformation. O'Leary (written commun., 2000) concurs that the Rock Valley fault zone and the Las Vegas Valley shear zone are kinematically related but that the relationship is too complex to accord with a conjugate origin. The anomalies generally track steeply dipping carbonates of the Bonanza King Formation and younger Ordovician formations, but Proterozoic clastic rocks, such as the Wood Canyon Formation, may be buried along this trend as well (C. Potter and D. Sweetkind, written commun., 1999). Such rocks are not typically magnetic, and the actual sources of the anomalies remain unknown.

Magnetic lineaments of the Rock Valley fault zone terminate at a pronounced circular magnetic anomaly (A, fig. 8) located directly south of Amargosa Valley. The dipolar nature and negative sense of the anomaly indicate that it originates from a reversely magnetized volcano or plug buried at very shallow depth beneath relatively nonmagnetic alluvial deposits. Based on its similarity with the magnetic anomaly over the Lathrop Wells basaltic center (L, fig. 8), Langenheim and others (1993) proposed that anomaly A is caused by a buried basaltic center. Computer models of the anomaly indicate that the volcanic center is less than 250 m beneath the topographic surface (Langenheim and others, 1993), a conclusion confirmed by subsequent drilling (Harris and others, 1992).

The location of anomaly A at the southern terminus of the Rock Valley fault zone may not be coincidental. Fractures within the fault zone may have promoted the ascension of magma to the surface. Although the Rock Valley fault zone exhibits mostly oblique displacement, the basaltic center beneath anomaly A suggests that extensional deformation may have been important in the Tertiary. We also note that anomaly A falls on the eastern margin of a regional-scale, north-striking trough in pre-Tertiary basement (fig. 10) interpreted from a three-dimensional gravity inversion (Blakely and others, 1998). A zone of north-trending magnetic lineaments north of anomaly A also follows the eastern margin of the basement trough, suggesting regional structural control (Blakely and others, 1998). This linear step in the pre-Tertiary basement has been referred to variously as the “gravity fault” (Connor and others, 2000) or Amargosa fault (Schweickert and Lahren, 1997).

Anomaly A is ringed on its northwestern and southwestern sides by six small, circular anomalies also probably caused by volcanoes or plugs buried at shallow depth. Models based on ground magnetic surveys over two of these anomalies (the two anomalies southwest of anomaly A) determined a maximum depth of 300 m below the surface (Langenheim, 1995).

A series of magnetic lineaments (R, fig. 8) radiates outward from anomaly A. These subtle features are only evident in residual magnetic anomalies (fig. 6). The radiating anomalies may be caused by small fractures or volcanic dikes associated with emplacement of the basaltic center beneath anomaly A. They also may express the southwestward continuation of the Rock Valley fault zone into the Amargosa Desert.

Funeral Range, Furnace Creek Wash, Greenwater Range, and surrounding areas

Pre-Cenozoic rocks of the Funeral Range are relatively nonmagnetic, as demonstrated by subdued magnetic patterns over most of the range (fig. 5). An exception occurs in the vicinity of Indian Pass (H, fig. 8), where a series of north- to north-northeast-striking anomalies completely cross the pre-Cenozoic exposures of the Funeral Range. Although low in amplitude, the short-wavelengths associated with these anomalies indicate that they originate from very near the topographic surface. The anomalies appear to coincide with a prominent set of north-northeast-striking faults that cut the Stirling Quartzite (C. Potter and D. Sweetkind, written commun., 1999). The position of the anomalies with respect to springs north of Furnace Creek (fig. 9) suggests that the faults may act as conduits for the flow of water from the north into Death Valley. Elsewhere, Stirling Quartzite is essentially nonmagnetic, and thus the ultimate source of the magnetic anomalies remains unclear. Volcanic rocks are exposed at both ends of the magnetic anomalies (fig. 9), and we speculate that the anomalies are caused by iron oxides leached from these volcanic rocks into underlying faults.

The Furnace Creek fault zone passes through Furnace Creek Wash as it leaves Death Valley to the southeast. This major crustal structure produces only a subtle magnetic pattern (F, fig. 8), which is most evident on the residual anomaly map (fig. 6). The subdued nature of the anomaly reflects, in part, the high altitude of the magnetic sensor over this location.

Volcanic rocks of the Greenwater Range produce a distinctive pattern of high-amplitude, short-wavelength magnetic anomalies (GR, fig. 8) characteristic of young volcanic rocks elsewhere. The rocks underlie the entire southwestern part of the aeromagnetic survey, including the Greenwater Valley, the western slopes of the Black Mountains, and parts of Furnace Creek Wash and the Amargosa Desert. The anomaly pattern is random in nature, although several prominent anomalies have northeastern and northwestern trends. Brown Peak (B, fig. 8) produces a complex magnetic anomaly with northeast strike, suggesting fault control along its northwestern margin. The eastern extent of these volcanic rocks is clearly demarcated by the aeromagnetic map as an extraordinarily abrupt change in magnetic pattern. Volcanic rocks in the subsurface extend as far east as Eagle Mountain and the southern end of the Resting Spring Range. In some localities, the eastern boundary may reflect the southeastern continuation of the Furnace Creek fault zone.

Two distinct magnetic anomalies are located within Chicago Valley (Ch, fig. 8). The western margin of the larger, southern anomaly lies over volcanic rocks mapped along the eastern margin of the Resting Spring Range. The lateral extent of the anomaly indicates where similar volcanic rocks are located at shallow depth in Chicago Valley.

Pahrump Valley, State Line fault zone, and surrounding areas

The State Line fault zone (Wright, 1988) in Pahrump Valley and Ash Meadows is a right-lateral, strike-slip zone of deformation that lies approximately parallel to the California-Nevada state line and within the Walker Lane belt. Wright (1988) proposed that Pahrump Valley and Ash Meadows are pull-apart basins, transtensional structures caused by right steps in the right-lateral State Line fault zone. Three-dimensional models based on gravity measurements (fig. 10, for example) support this interpretation but indicate complex basement structures beneath both Pahrump Valley and Ash Meadows (Blakely and others, 1998, 1999). Pahrump Valley is underlain by two deep, isolated sub-basins lying astride the state line. The intervening basement ridge is apparently a horst-like structure caught between strands of the State Line fault zone. A similar ridge beneath Ash Meadows also separates several sub-basins and is on strike with the Pahrump Valley ridge.

Magnetic anomalies over Pahrump Valley are very subdued, as expected for an alluvial-filled basin. Subtle magnetic anomalies do exist, however, as demonstrated by the residual magnetic anomaly map (fig. 6). A cluster of magnetic lineaments (SLFZ, fig. 8) follows the State Line fault in Pahrump Valley, where some of the individual anomalies correspond to

Quaternary faults mapped by Hoffard (1991) and Lundstrom and others (2000). This general pattern of anastomizing magnetic lineaments continues northwestward along the state line at least as far north as latitude 36°30’N., a distance of over 100 km (62 mi). Most of these lineaments lie over alluvium not expected to be magnetic, and thus the actual magnetic sources remain problematic. At various places, the anomalies may reflect underlying magnetic lithologies, reworked magnetite-bearing sediments in ancient fluvial systems, or alteration along fractures or faults.

Several magnetic lineaments (D, fig. 8) veer northward from the State Line fault zone, pass near Devils Hole, and terminate near the Rock Valley fault zone. Although perhaps not kinematically related, this set of anomalies may indicate a hydrologic connection between the Rock Valley fault zone, Devils Hole, and the State Line fault. The alignments of springs along magnetic anomalies in Pahrump Valley and near Devils Hole (fig. 9) suggest that these anomalies are caused by faults in the alluvium that influence ground-water flow.

A cluster of low-amplitude, short-wavelength magnetic anomalies lies over alluvium northeast of Devils Hole (J, fig. 8). These anomalies reflect sources very near the topographic surface. Although no volcanic rocks crop out in the vicinity, the random nature of the anomaly pattern is suggestive of volcanic rocks at shallow depth. This interpretation is supported by independent subsurface information based on wells (Johnston, 1968) and seismic reflection (Brocher and others, 1993).

CONCLUSION

High-resolution aeromagnetic data from the Amargosa Desert, Pahrump Valley, Funeral Range, Furnace Creek Wash, Greenwater Valley, and Greenwater Range reflect diverse lithologies at and below the topographic surface. These data have permitted a preliminary interpretation of the faults and underlying lithologies of the region that we believe will be important in ongoing geologic and hydrologic investigations.

ACKNOWLEDGMENTS

This report benefited greatly from reviews by E.H. McKee and Meghan Anderson. Helpful comments also were provided by Dennis O'Leary, Chris Potter, and Don Sweetkind. Nick Stellavato was instrumental in providing logistical support during the aeromagnetic survey. We are also grateful to Martin Bates and Sander Geophysics Limited for the data acquisition and initial data processing.

REFERENCES

Baldwin, M.J., and Jahren, C.E., 1982, Magnetic properties of drill core and surface samples from the Calico Hills area, Nye County, Nevada: U.S. Geological Survey Open-File Report 82–536, 27 p.

Bath, G.D., and Jahren, C.E., 1984, Interpretations of magnetic anomalies at a potential repository site located in the Yucca Mountain area, Nevada Test Site: U.S. Geological Survey Open-File Report 84–120, 40 p.

Blakely, R.J., 1995, Potential Theory in Gravity and Magnetic Applications: Cambridge University Press, 441 p.

Blakely, R.J., Jachens, R.C., Calzia, J.P., and Langenheim, V.E., 1999, Cenozoic basins of the Death Valley extended terrane as reflected in regional-scale gravity anomalies, *in* Wright, L.A., and Troxel, B.W., eds., Cenozoic basins of the Death Valley region: Geological Society of America Special Paper 333, p. 1–16, scale 1:1,000,000.

Blakely, R.J., Morin, R.L., McKee, E.H., Schmidt, K.M., Langenheim, V.E., and Dixon, G.L., 1998, Three-dimensional model of Paleozoic basement beneath Amargosa Desert and Pahrump Valley, California and Nevada: Implications for tectonic evolution and water resources: U.S. Geological Survey Open-File Report 98–496, 31 p.

Blakely, R.J., and Simpson, R.J., 1986, Approximating edges of source bodies from magnetic or gravity anomalies: Geophysics, v. 51, p. 1494–1498.

Blank, H.R., 1987, Role of regional aeromagnetic and gravity data in mineral-resource investigations, southeastern Nevada, USGS Research on Mineral Resources—1987, Third Annual V.E. McKelvey Forum on Mineral and Energy Resources: U.S. Geological Survey Circular 995, p. 5-6.

Brocher, T.M., Carr, M.D., Fox, K.F., Jr., and Hart, P.E., 1993, Seismic-reflection profiling across Tertiary extensional structures in the eastern Amargosa Desert, southern Nevada, Basin and Range province: Geological Society of America Bulletin, v. 105, p. 30–46.

Connor, C.B., Stamatakos, J.A., Ferrill, D.A., Hill, B.E., Ofoegbu, G.I., Conway, F.M., Sagar, B., and Trapp, J., 2000, Geologic factors controlling patterns of small-volume basaltic volcanism: Application to a volcanic hazards assessment at Yucca Mountain, Nevada: Journal of Geophysical Research, v. 105, p. 417–432.

Dettinger, M.D., 1989, Distribution of carbonate-rock aquifers in southern Nevada and the potential for their development, summary of findings, 1985-88: Program for the Study and Testing of Carbonate-Rock Aquifers in Eastern and Southern Nevada, Summary Report No. 1, U.S. Geological Survey, Desert Research Institute, and University of Nevada.

Dobrin, M.B., and Savit, C.H., 1988, Introduction to Geophysical Prospecting: McGraw-Hill Book Company, 867 p.

Hamilton, W.B., 1988, Detachment faulting in the Death Valley region, California and Nevada, *in* Carr, M.D., and Yount, J.C., eds., Geologic and hydrologic investigations of a potential nuclear waste disposal site at Yucca Mountain, southern Nevada: U.S. Geological Survey Bulletin 1790, p. 51–85.

Harris, A.G., Repetski, J.E., Clayton, J.L., Grow, J.A., Carr, M.D., and Daws, T.A., 1992, Results from 1991 wildcat wells near Yucca Mountain, Nevada: Geological Society of America Abstracts with Programs, Rocky Mountain section, v. 24, p. 17.

Hildenbrand, T.G., and Kucks, R.P., 1988, Total intensity magnetic anomaly map of Nevada: Nevada Bureau of Mines and Geology Map 93A, scale 1:750,000.

Hoffard, J.L., 1991, Quaternary tectonics and basin history of Pahrump and Stewart Valley, Nevada and California: University of Nevada, Reno, M.S. thesis, 138 p., 5 plates.

Jennings, C.W., 1977, Geologic map of California: California Division of Mines and Geology Geologic Map No. 2, scale 1:750,000.

Johnston, R.H., 1968, U.S. Geological Survey tracer study, Amargosa Desert, Nye County, Nevada, Part I: Exploratory drilling, tracer well construction and testing and preliminary findings: U.S. Geological Survey Open-File Report, 64 p.

Laczniak, R.J., Cole, J.C., Sawyer, D.A., and Trudeau, D.A., 1996, Summary of hydrogeologic controls on ground-water flow at the Nevada Test Site, Nye County, Nevada: U.S. Geological Survey Water Resources Investigations Report 96–4109, 59 p.

Langenheim, V.E., 1995, Magnetic and gravity studies of buried volcanic centers in the Amargosa Desert and Crater Flat, southwest Nevada: U.S. Geological Survey Open-File Report 95–564, 36 p.

Langenheim, V.E., Kirchoff-Stein, K.S., and Oliver, H.W., 1993, Magnetic investigations of buried volcanic centers near Yucca Mountain, Nevada: American Nuclear Society Proceedings of the Fourth Annual International Conference on High-Level Waste Management, v. 2, p. 1840-6.

Louie, J., Shields, G., Hasting, M., Plank, G., and Bowman, S., 1998, Shallow geophysical constraints on displacement and segmentation of the Pahrump Valley fault zone, California–Nevada border, *in* Lund, W.R., ed., Proceedings of the Basin and Range Province Seismic Hazards Summit, May 13-15, 1997: Utah Geological Survey, Cedar City, Utah.

Lundstrom, S.C., Mahan, S.A., Blakely, R.J., Paces, J.B., Young, O.D., and Dixon, G.L., 2000, Geologic map of the Mound Spring Quadrangle, Nye and Clark Counties, Nevada, and Inyo County, California: U.S. Geological Survey Miscellaneous Field Investigations Map, scale 1:24,000 with text, in press.

McKee, E.H., 1997, Evaluation of geologic structure guiding ground water flow south and west of Frenchman Flat, Nevada Test Site: U.S. Geological Survey Open-File Report 97–734, 26 p.

Monsen, S.A., Carr, M.D., Reheis, M., and Orkild, P.J., 1992, Geologic map of Bare Mountain, Nye County, Nevada: U.S. Geological Survey Miscellaneous Investigations Map I–2201, scale 1:24,000, 6 p.

O'Leary, D.W., Tectonic significance of the Rock Valley fault zone, Nevada Test Site, 2000, *in* ???, in press.

Ponce, D.A., 1984, Gravity and magnetic evidence for a granitic intrusion near Wahmonie site, Nevada Test Site, Nevada: Journal of Geophysical Research, v. 89, p. 9401–9413.

Ponce, D.A., 1993, Geophysical investigations of concealed faults near Yucca Mountain, southwest Nevada: American Nuclear Society Proceedings of the Fourth Annual International Conference on High Level Waste Management, v. 1, p. 168–174.

Ponce, D.A., 1996, Interpretive geophysical fault map across the central block of Yucca Mountain, Nevada: U.S. Geological Survey Open-File Report 96–285, 15 p., 4 plates.

Ponce, D.E., Kohrn, S.B., and Waddell, S., 1992, Gravity and magnetic data of Fortymile Wash, Nevada Test Site, Nevada: U.S. Geological Survey Open-File Report 92–343, 33 p.

Ponce, D.A., and Langenheim, V.E., 1994, Preliminary gravity and magnetic models across Midway Valley and Yucca Wash, Nevada: U.S. Geological Survey Open-File Report 94–572, 25 p.

Ponce, D.A., Sikora, R.F., Roberts, C.W., Morin, R.L., and Halvorson, P.F., 1995, Magnetic investigations along selected high-resolution seismic traverses in the central block of Yucca Mountain, Nevada: U.S. Geological Survey Open-File Report 95–667, 23 p.

Roberts, C.W., and Jachens, R.C., 1999, Preliminary aeromagnetic anomaly map of California: U.S. Geological Survey Open-File Report 99–440, 14 p., scale 1:5,600,000, http://geopubs.wr.usgs.gov/open-file/of99-440.

Rosenbaum, J.G., Hudson, M.R., and Scott, R.B., 1991, Paleomagnetic constraints on the geometry and timing of deformation at Yucca Mountain, Nevada: Journal of Geophysical Research, v. 96, p. 1963–1979.

Rowley, P., 1998, Cenozoic transverse zones and igneous belts in the Great Basin, western United States: Their tectonic and economic implications, *in* Faulds, J.E., and Stewart, J.H., eds., Accommodation Zones and Transfer Zones: The Regional Segmentation of the Basin and Range Province: Boulder, Colorado, Geological Society of America Special Paper 323, p. 195–228.

Schweickert, R.A., and Lahren, M.M., 1997, Strike-slip fault system in Amargosa Valley and Yucca Mountain, Nevada: Tectonophysics, v. 272, p. 25–41.

Stewart, J.H., 1983, Extensional tectonics in the Death Valley area, California: Transport of the Panamint Range structural block 80 km northwestward: Geology, v. 11, p. 153–157.

Stewart, J.H., and Carlson, J.E., 1978, Geologic map of Nevada: U.S. Geological Survey, scale 1:500,000.

Simonds, F.W., Whitney, J.W., Fox, K.F., Ramelli, A.R., Yount, J.C., Carr, M.D., Menges, C.M., Dickerson, R.P., and Scott, R.B., 1995, Map showing fault activity in theYucca Mountain area, Nye County, Nevada: U.S. Geological Survey Map I-2520, 1:24,000 scale.

Stamatakos, J.A., Connor, C.B., Hill, B.E., Lane Magsino, L., and Ferrill, D.A., 1997, The Carrara fault in southwestern Nevada revealed from detailed gravity and magnetic results: Implications for seismicity, volcanism, and tectonics near Yucca Mountain, Nevada: EOS, Transactions of the American Geophysical Union, v. 86, Fall Meeting Supplement, p. F453.

Wernicke, B., Axen, G.J., and Snow, J.K., 1988, Basin and Range extensional tectonics at the latitude of Las Vegas, Nevada: Geological Society of America Bulletin, v. 100, p. 1738–1757.

Winograd, I.J., and Thordarson, W., 1975, Hydrogeologic and hydrochemical framework, south-central Great Basin, Nevada-California, with special reference to the Nevada Test Site: U.S. Geological Survey Professional Paper 712–C, 126 p.

Wright, L.A., 1988, Overview of the role of strike-slip and normal faulting in the Neogene history of the region northeast of Death Valley, California-Nevada, *in* Ellis, M.A., ed., Selected papers from the workshop, Late Cenozoic evolution of the southern Great Basin, Reno, Nevada, November 10-13, 1987, p. 1–11.

Langenheim, V.E., Kirchoff-Stein, K.S., and Oliver, H.W., 1993, Magnetic investigations of buried volcanic centers near Yucca Mountain, Nevada: American Nuclear Society Proceedings of the Fourth Annual International Conference on High-Level Waste Management, v. 2, p. 1840-6.

Louie, J., Shields, G., Hasting, M., Plank, G., and Bowman, S., 1998, Shallow geophysical constraints on displacement and segmentation of the Pahrump Valley fault zone, California–Nevada border, *in* Lund, W.R., ed., Proceedings of the Basin and Range Province Seismic Hazards Summit, May 13-15, 1997: Utah Geological Survey, Cedar City, Utah.

Lundstrom, S.C., Mahan, S.A., Blakely, R.J., Paces, J.B., Young, O.D., and Dixon, G.L., 2000, Geologic map of the Mound Spring Quadrangle, Nye and Clark Counties, Nevada, and Inyo County, California: U.S. Geological Survey Miscellaneous Field Investigations Map, scale 1:24,000 with text, in press.

McKee, E.H., 1997, Evaluation of geologic structure guiding ground water flow south and west of Frenchman Flat, Nevada Test Site: U.S. Geological Survey Open-File Report 97–734, 26 p.

Monsen, S.A., Carr, M.D., Reheis, M., and Orkild, P.J., 1992, Geologic map of Bare Mountain, Nye County, Nevada: U.S. Geological Survey Miscellaneous Investigations Map I–2201, scale 1:24,000, 6 p.

O'Leary, D.W., Tectonic significance of the Rock Valley fault zone, Nevada Test Site, 2000, *in* ???, in press.

Ponce, D.A., 1984, Gravity and magnetic evidence for a granitic intrusion near Wahmonie site, Nevada Test Site, Nevada: Journal of Geophysical Research, v. 89, p. 9401–9413.

Ponce, D.A., 1993, Geophysical investigations of concealed faults near Yucca Mountain, southwest Nevada: American Nuclear Society Proceedings of the Fourth Annual International Conference on High Level Waste Management, v. 1, p. 168–174.

Ponce, D.A., 1996, Interpretive geophysical fault map across the central block of Yucca Mountain, Nevada: U.S. Geological Survey Open-File Report 96–285, 15 p., 4 plates.

Ponce, D.E., Kohrn, S.B., and Waddell, S., 1992, Gravity and magnetic data of Fortymile Wash, Nevada Test Site, Nevada: U.S. Geological Survey Open-File Report 92–343, 33 p.

Ponce, D.A., and Langenheim, V.E., 1994, Preliminary gravity and magnetic models across Midway Valley and Yucca Wash, Nevada: U.S. Geological Survey Open-File Report 94–572, 25 p.

Ponce, D.A., Sikora, R.F., Roberts, C.W., Morin, R.L., and Halvorson, P.F., 1995, Magnetic investigations along selected high-resolution seismic traverses in the central block of Yucca Mountain, Nevada: U.S. Geological Survey Open-File Report 95–667, 23 p.

Roberts, C.W., and Jachens, R.C., 1999, Preliminary aeromagnetic anomaly map of California: U.S. Geological Survey Open-File Report 99–440, 14 p., scale 1:5,600,000, http://geopubs.wr.usgs.gov/open-file/of99-440.

Rosenbaum, J.G., Hudson, M.R., and Scott, R.B., 1991, Paleomagnetic constraints on the geometry and timing of deformation at Yucca Mountain, Nevada: Journal of Geophysical Research, v. 96, p. 1963–1979.

Rowley, P., 1998, Cenozoic transverse zones and igneous belts in the Great Basin, western United States: Their tectonic and economic implications, *in* Faulds, J.E., and Stewart, J.H., eds., Accommodation Zones and Transfer Zones: The Regional Segmentation of the Basin and Range Province: Boulder, Colorado, Geological Society of America Special Paper 323, p. 195–228.

Schweickert, R.A., and Lahren, M.M., 1997, Strike-slip fault system in Amargosa Valley and Yucca Mountain, Nevada: Tectonophysics, v. 272, p. 25–41.

Stewart, J.H., 1983, Extensional tectonics in the Death Valley area, California: Transport of the Panamint Range structural block 80 km northwestward: Geology, v. 11, p. 153–157.

Stewart, J.H., and Carlson, J.E., 1978, Geologic map of Nevada: U.S. Geological Survey, scale 1:500,000.

Simonds, F.W., Whitney, J.W., Fox, K.F., Ramelli, A.R., Yount, J.C., Carr, M.D., Menges, C.M., Dickerson, R.P., and Scott, R.B., 1995, Map showing fault activity in theYucca Mountain area, Nye County, Nevada: U.S. Geological Survey Map I-2520, 1:24,000 scale.

Stamatakos, J.A., Connor, C.B., Hill, B.E., Lane Magsino, L., and Ferrill, D.A., 1997, The Carrara fault in southwestern Nevada revealed from detailed gravity and magnetic results: Implications for seismicity, volcanism, and tectonics near Yucca Mountain, Nevada: EOS, Transactions of the American Geophysical Union, v. 86, Fall Meeting Supplement, p. F453.

Wernicke, B., Axen, G.J., and Snow, J.K., 1988, Basin and Range extensional tectonics at the latitude of Las Vegas, Nevada: Geological Society of America Bulletin, v. 100, p. 1738–1757.

Winograd, I.J., and Thordarson, W., 1975, Hydrogeologic and hydrochemical framework, south-central Great Basin, Nevada-California, with special reference to the Nevada Test Site: U.S. Geological Survey Professional Paper 712–C, 126 p.

Wright, L.A., 1988, Overview of the role of strike-slip and normal faulting in the Neogene history of the region northeast of Death Valley, California-Nevada, *in* Ellis, M.A., ed., Selected papers from the workshop, Late Cenozoic evolution of the southern Great Basin, Reno, Nevada, November 10-13, 1987, p. 1–11.

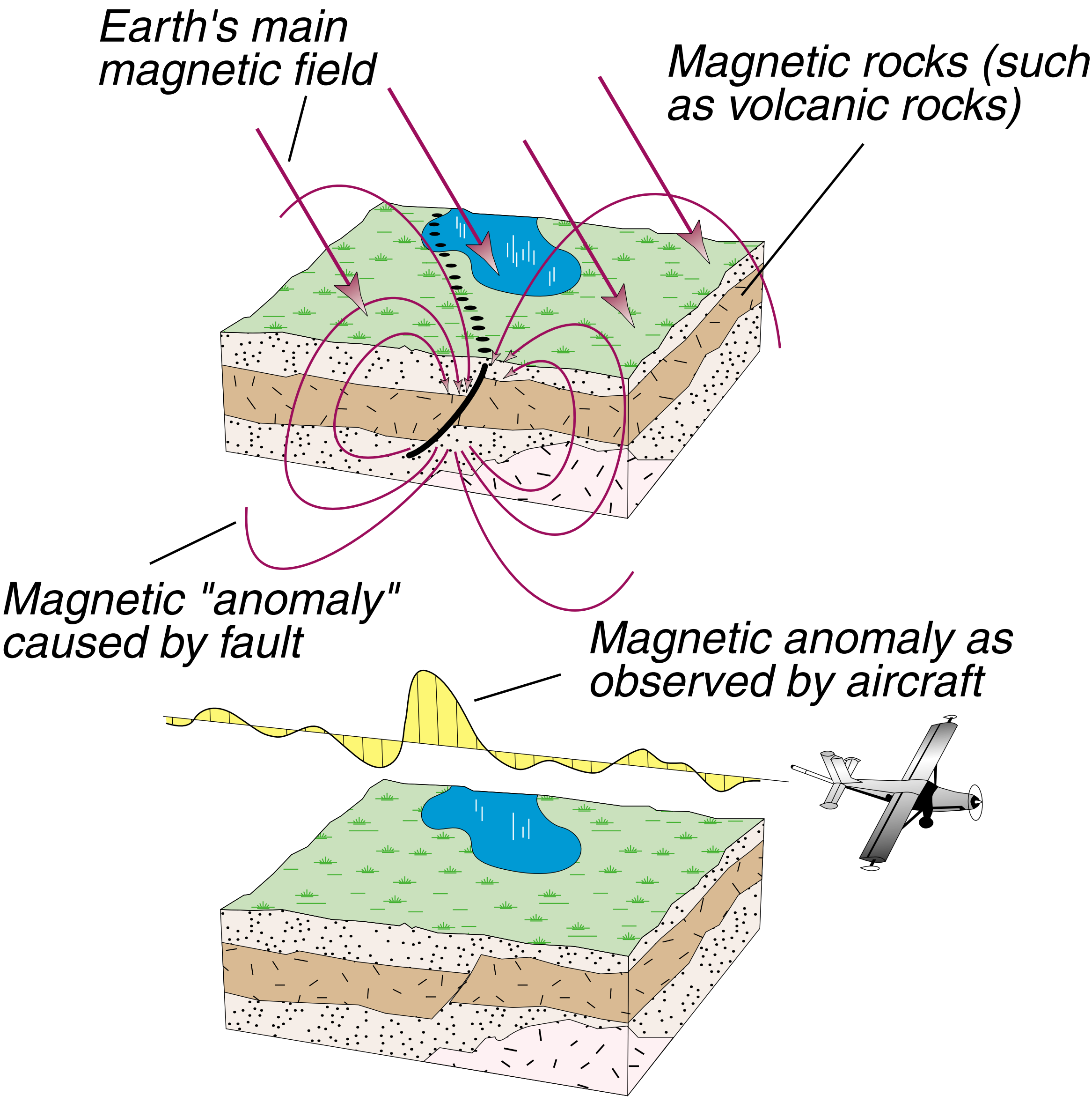

Figure 1.—Cartoon illustration of the magnetic method. Magnetic rocks (such as the faulted volcanic unit shown here) produce small magnetic fields that perturb the much larger field originating from the earth's core. Much can be learned about magnetic rocks by measuring the magnetic field near the topographic surface, even though those rocks may be completely concealed.

Terrain

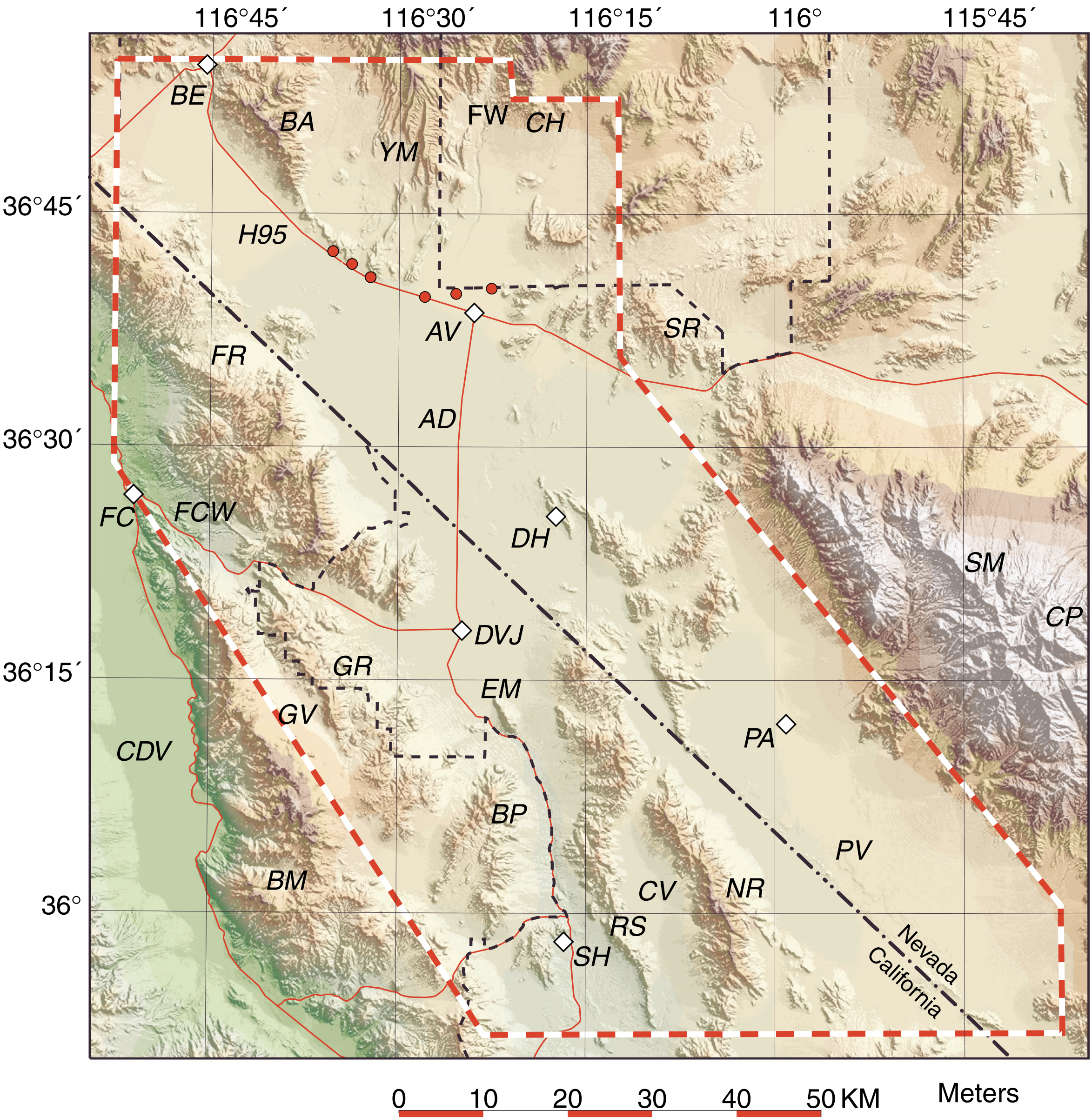

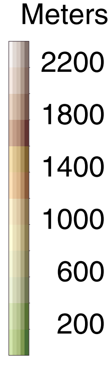

Figure 2.—Boundaries of aeromagnetic survey (red and white dashed line) shown on topographic map. Black dashed lines show the Nevada Test Site (northern part of map) and Death Valley National Park (western part of map). Solid red lines are major roads. Red dots show the location of Nye County Early Warning Drilling Project boreholes. AD, Amargosa Desert; AV, Amargosa Valley; BE, Beatty; BA, Bare Mountain; BM, Black Mountains; BP, Brown Peak; CDV, central Death Valley; CH, Calico Hills; CP, Charleston Peak; CV, Chicago Valley; DH, Devils Hole; DVJ, Death Valley Junction; EM, Eagle Mountain; FC, Furnace Creek; FCW, Furnace Creek Wash; FR, Funeral Range; GR, Greenwater Range; GV, Greenwater Valley; H95, U.S. Highway 95; NR, Nopah Range; PA, Pahrump; PV, Pahrump Valley; RS, Resting Spring Range; SH, Shoshone; SM, Spring Mountains; SR, Specter Range; YM, Yucca Mountain.

Generalized Geology

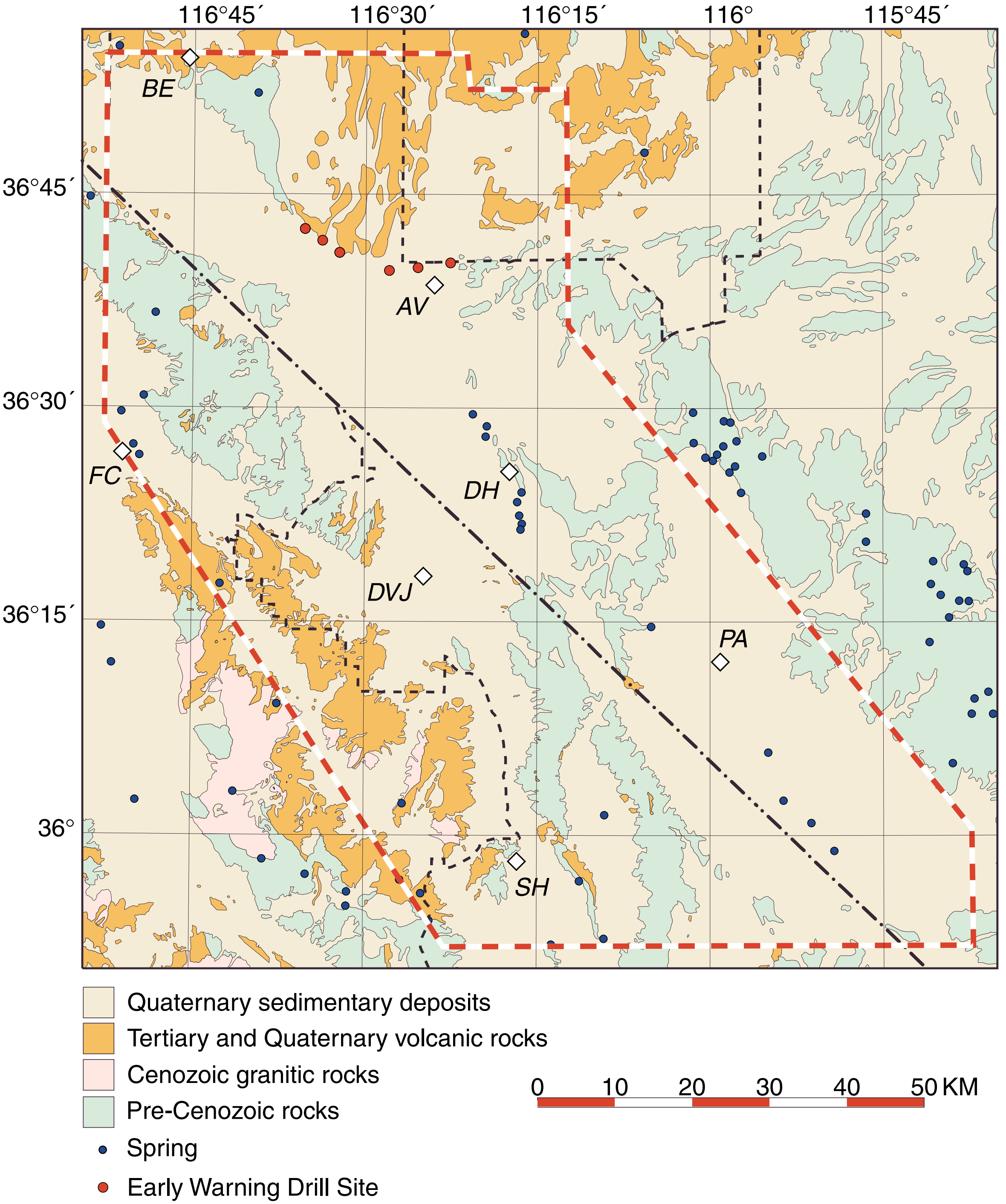

Figure 3.—Boundaries of aeromagnetic survey on generalized geologic map. See caption to figure 2 for description of dashed lines and abbreviations. Geology simplified from statewide compilations of California (Jennings, 1977) and Nevada (Stewart and Carlson, 1978). Springs are from 1:250,000-scale U.S. Geological Survey topographic maps.

Flight Path

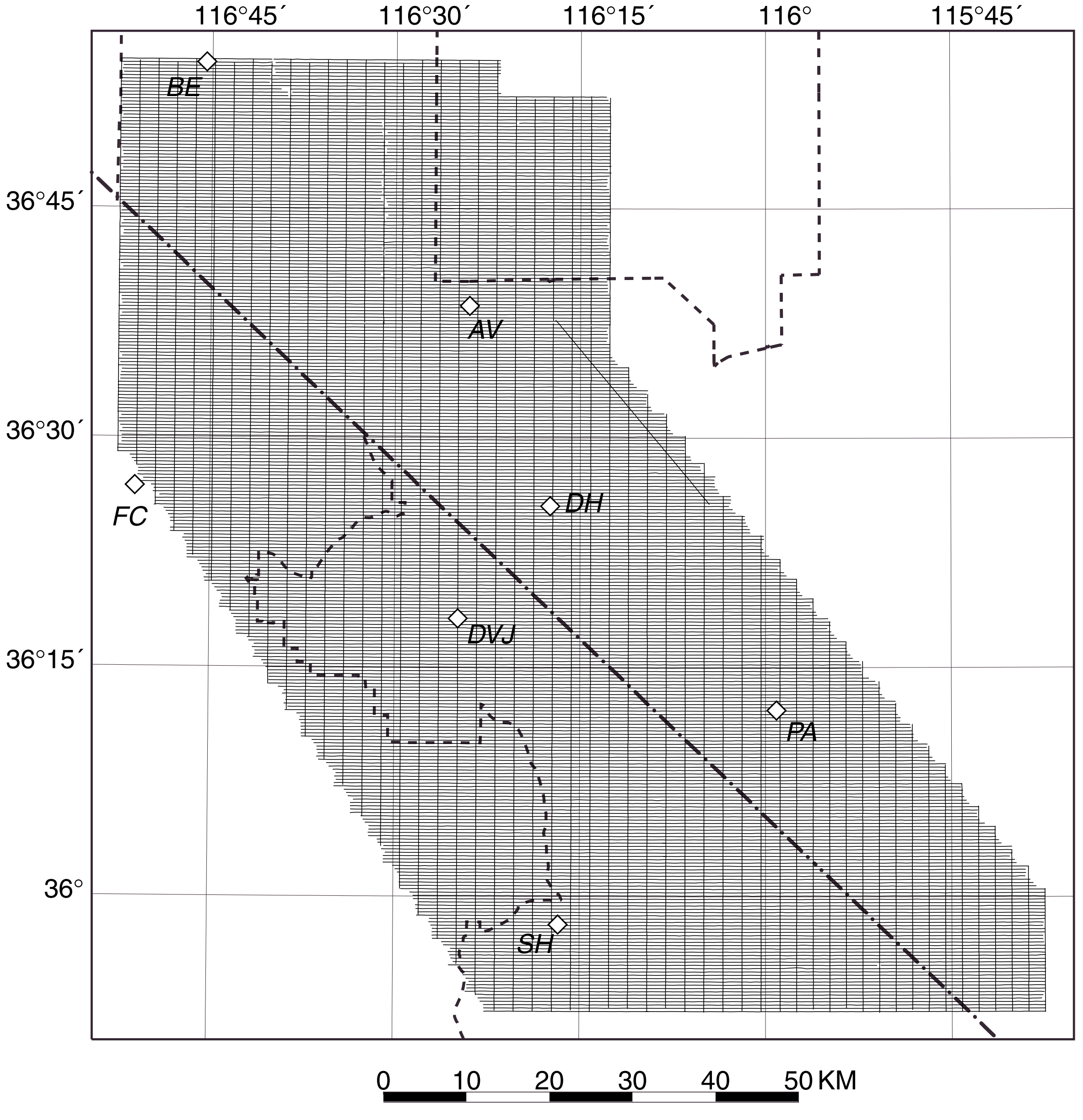

Figure 4.—Flight line and tie line map. The black lines on this map indicate the aircraft flight-path. Flight lines were oriented east-west and spaced 400 m apart. North-south tie lines were spaced 2.3 km (1.4 mi) apart. Flight altitude was 150 m (500 ft) above terrain, or as low as permitted by aircraft safety. Total distance flown was 23,333 km (14,502 mi). See figure 2 for description of dashed lines and abbreviations.

Aeromagnetic Anomalies

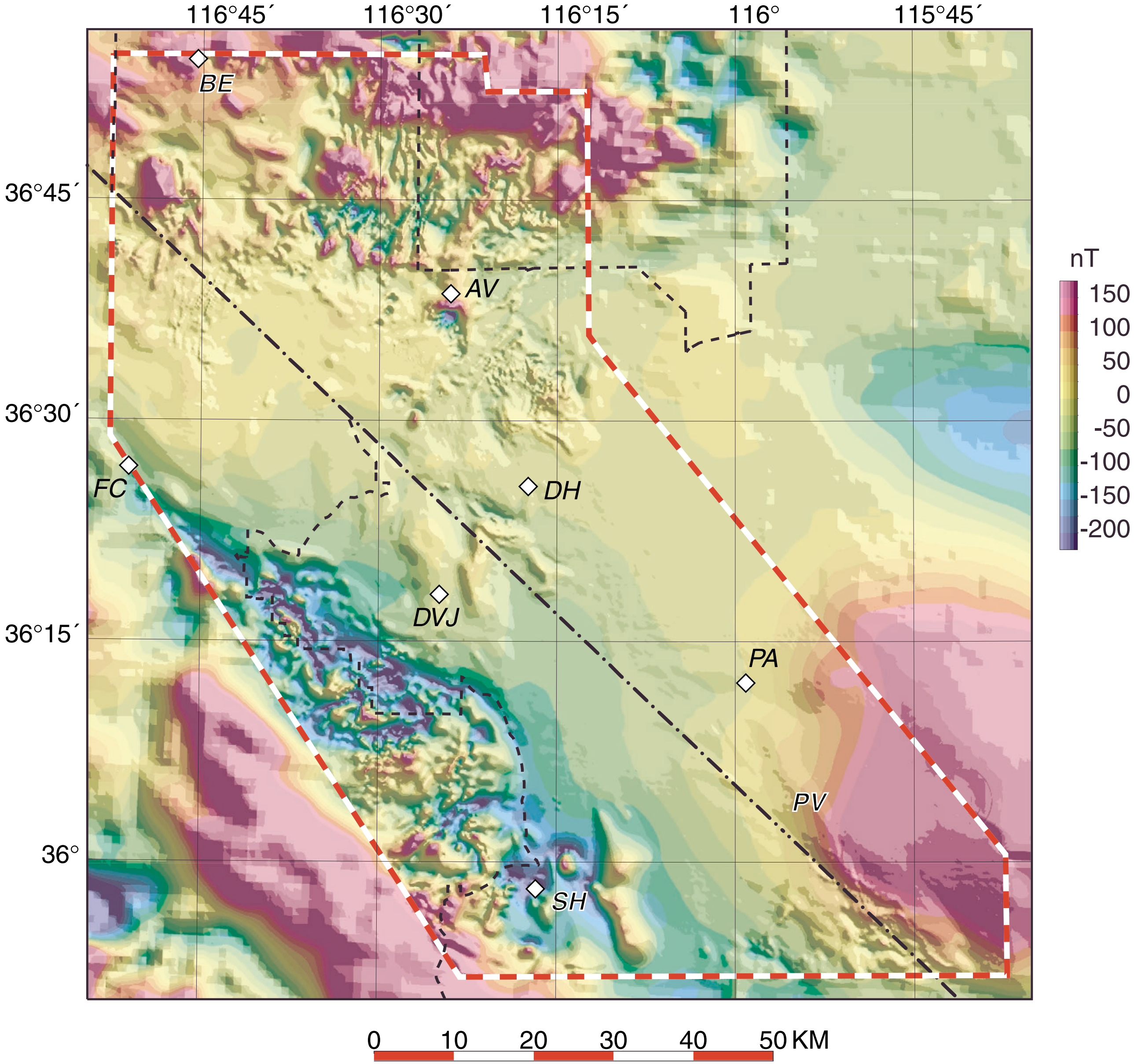

Figure 5.— Aeromagnetic anomaly map. The colors on this map indicate the intensity of the earth's magnetic field relative to a global standard, which in turn reflects the magnetization of the upper part of the earth's crust. The red-and-white dashed line indicates the boundary of the Amargosa aeromagnetic survey. Aeromagnetic anomalies outside of this boundary in Nevada are from Hildenbrand and Kucks (1988) and in California from Roberts and Jachens (1999). See figure 2 for description of other dashed lines and abbreviations. Near-surface volcanic rocks cause the high frequency anomalies in the northern and southwestern parts of the map. The large anomaly in the southeastern part of the map is thought to be caused by Precambrian rocks at significant depth. More difficult to explain are the subtle magnetic anomalies over sediment-filled basins (like Pahrump Valley), as these sedimentary deposits are not typically magnetic.

Residual Magnetic Anomaly

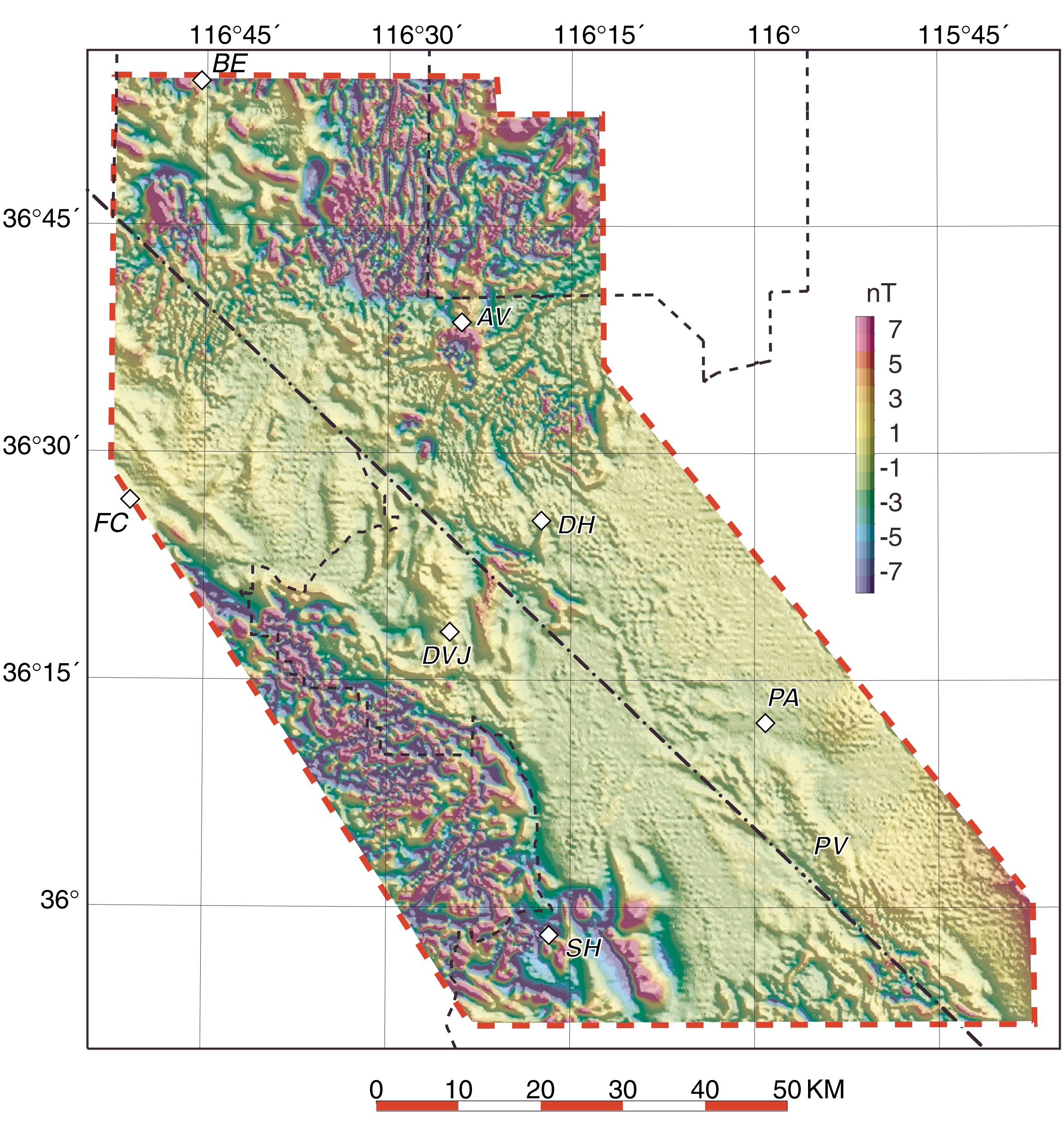

Figure 6.— Residual anomaly map. This map shows the aeromagnetic data processed in such a way as to emphasize shallow magnetic sources. See text for explanation of methodology and figure 2 for description of dashed lines and abbreviations.

Magnetization Boundaries

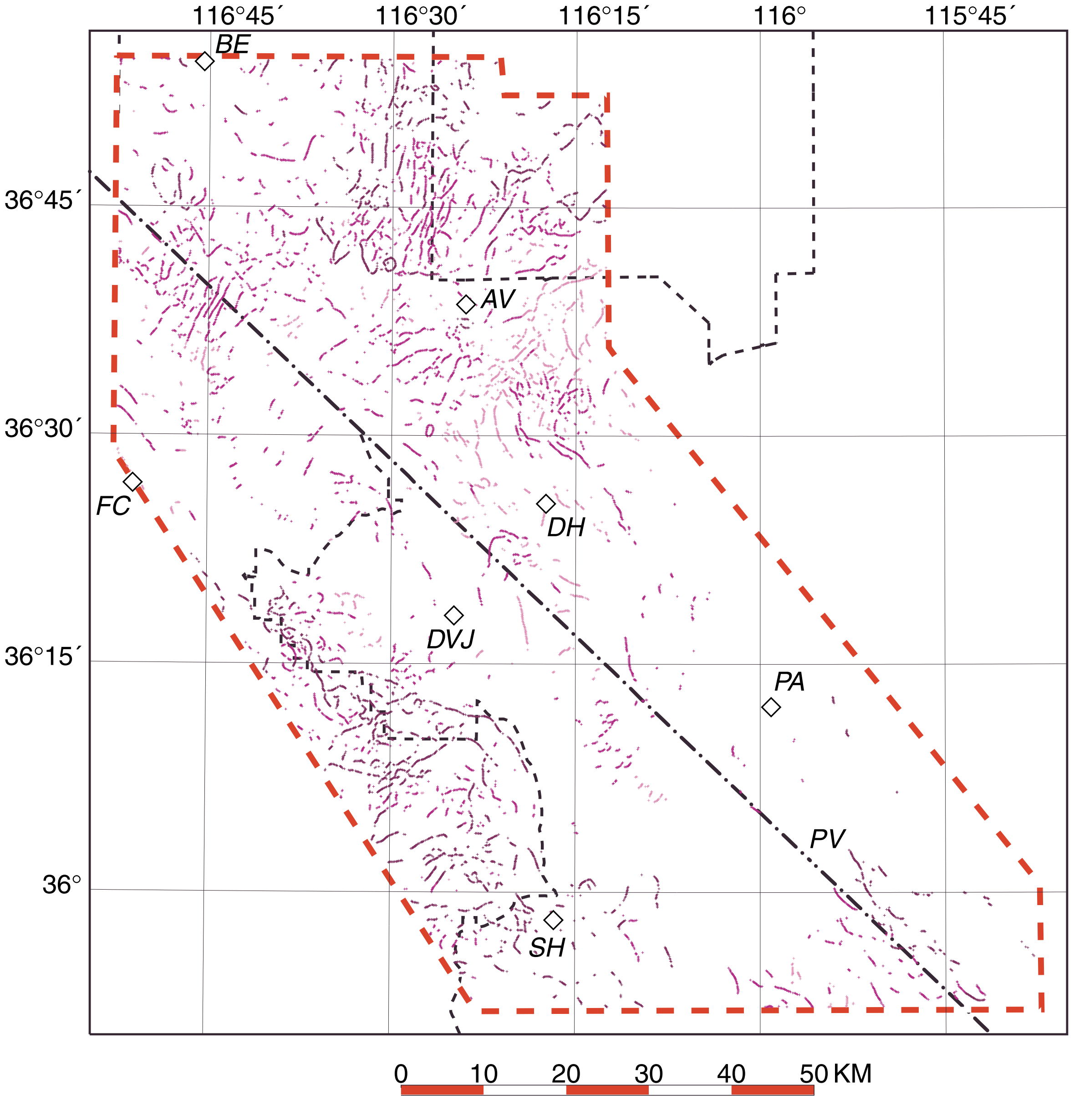

Figure 7.—Magnetic boundary map. Symbols on this map indicate magnetic contacts automatically calculated from the aeromagnetic data. See Blakely and Simpson (1986) for discussion about the assumptions and limitations behind this method. See figure 2 for description of dashed lines and abbreviations.

Interpretation

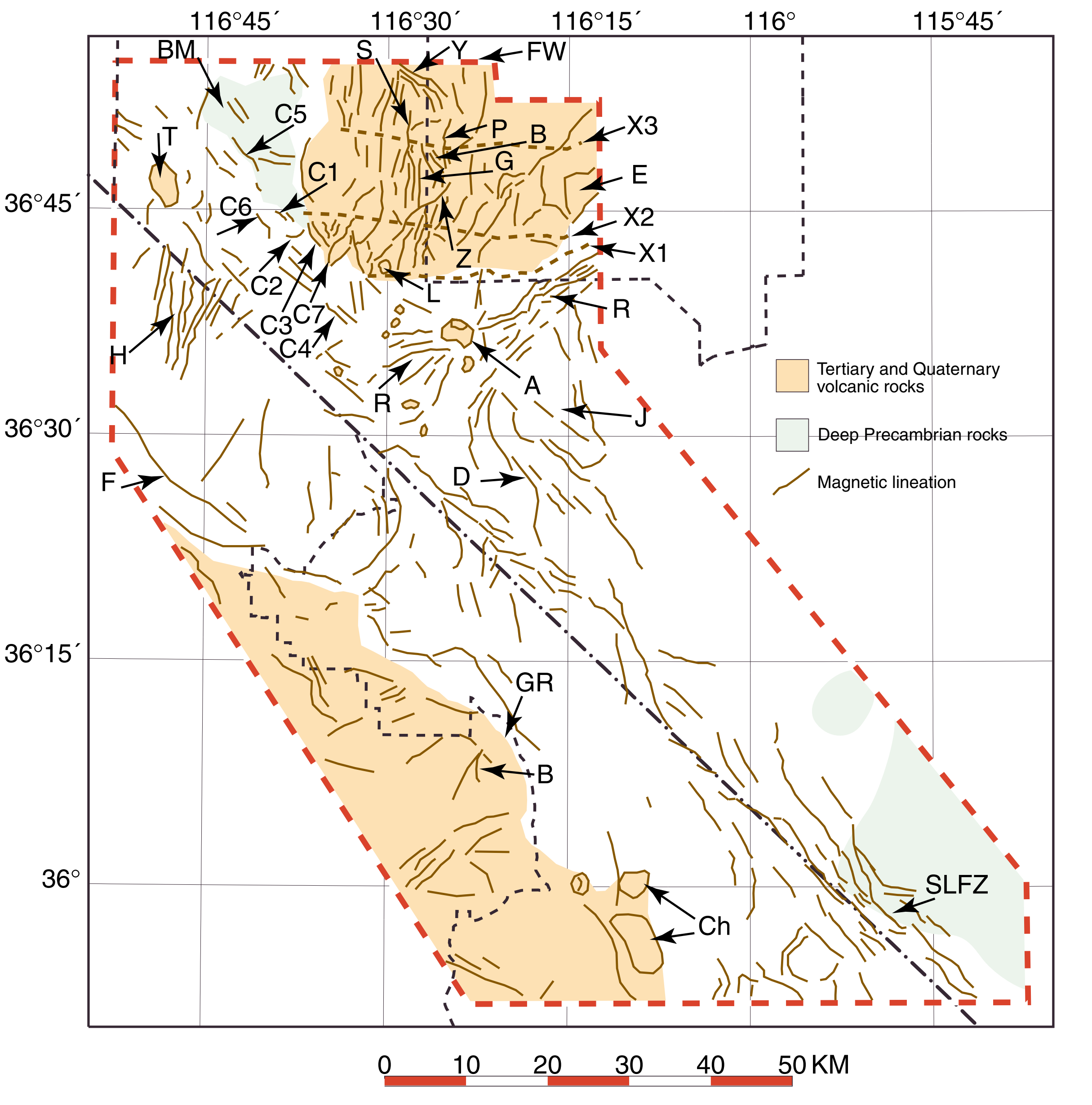

Figure 8.—Interpretation of aeromagnetic anomalies. Lines indicate magnetic anomalies and lineaments, some of which are caused by shallow faults. Colored patterns indicate the location of specific lithologies in the subsurface. Letters point to anomalies and patterns discussed in text. See figure 2 for description of dashed lines.

Magnetic Lineations on Generalized Geology

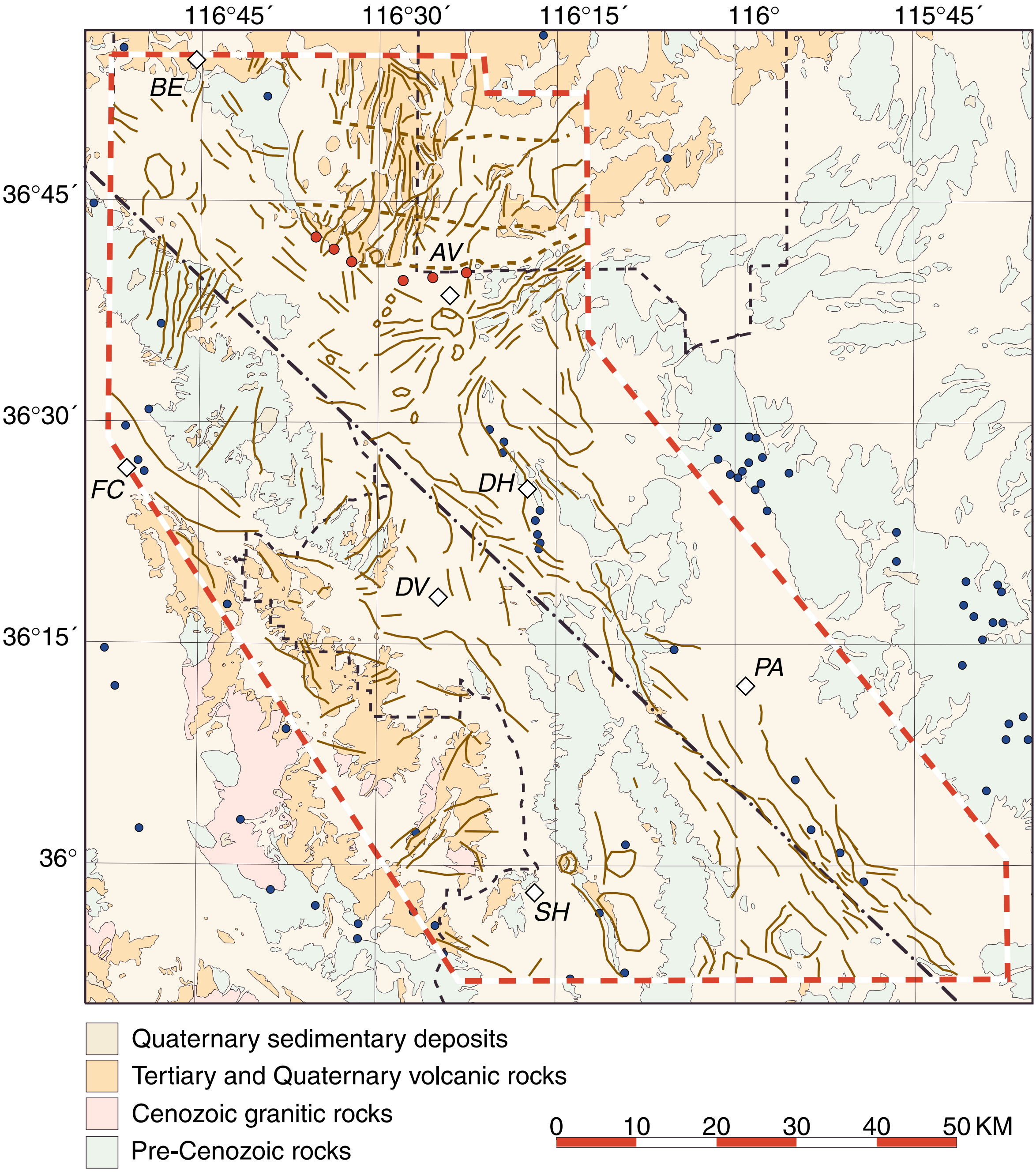

Figure 9.—Interpretation of magnetic lineaments (from fig. 8) superimposed on generalized geologic map. See caption to figure 3 for geology citations and explanation of other symbols. See figure 2 for description of dashed lines and abbreviations.

Magnetic Lineations on Basement Surface

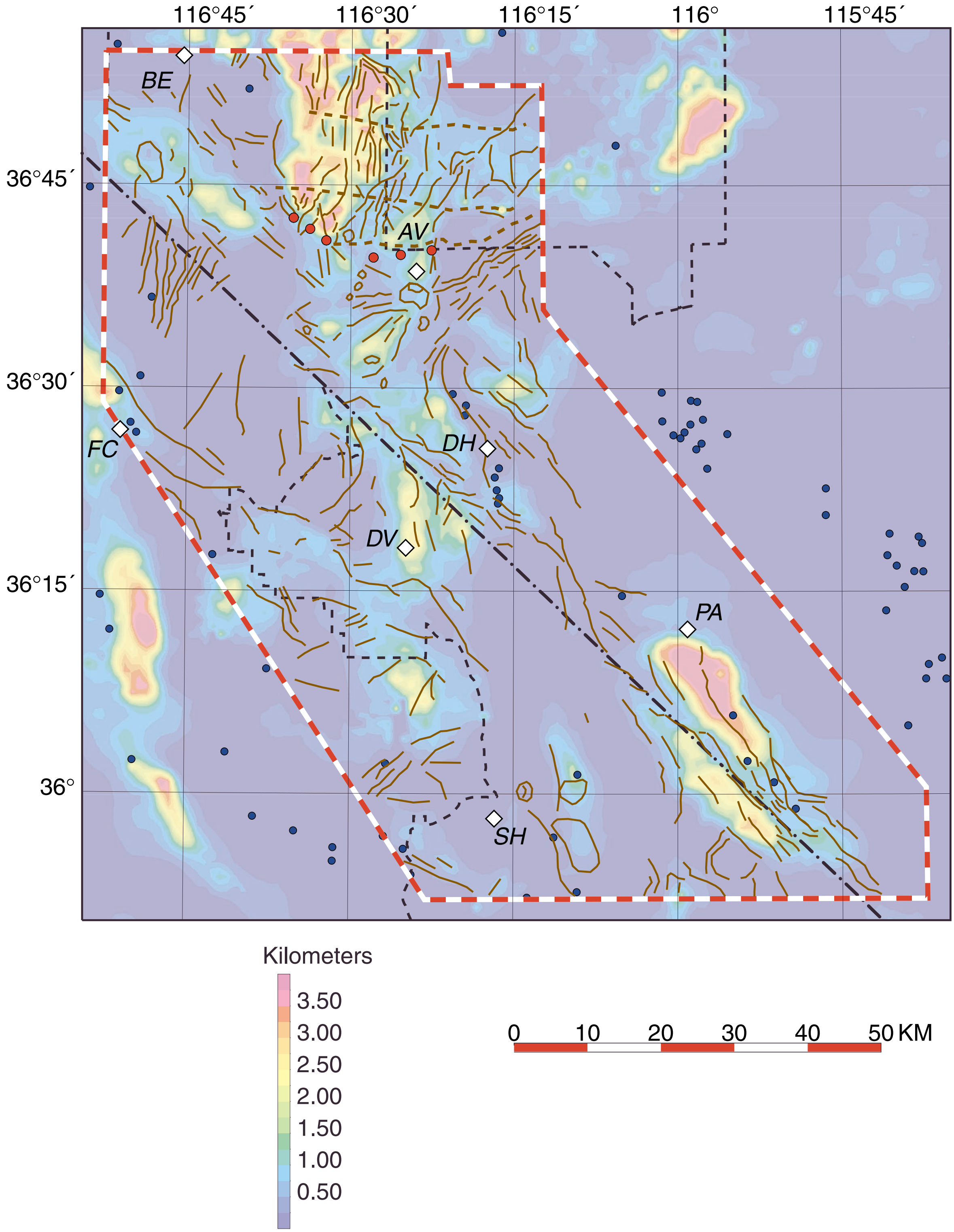

Figure 10.—Interpretation of magnetic lineaments (from fig. 8) superimposed on depth to pre-Tertiary basement. The basement surface was determined with a three-dimensional inversion of gravity data, constrained by geologic mapping, well information, and seismic-reflection data (Blakely and others, 1998). See figure 2 for description of dashed lines and abbreviations.